A Novel Method for Experimental Fault Simulation and Remaining Useful Life Estimation in Bearings

Pedro Fernando Poveda
Departamento de Mecânica (DME)
Instituto Federal de Educação, Ciência e Tecnologia de São Paulo (IFSP)
São Paulo/SP, Brasil
poveda@ifsp.edu.br

Marcos Rodrigues de Carvalho
Centro do Reator de Pesquisas (CERPQ)
Instituto de Pesquisas Energéticas e Nucleares (IPEN)
São Paulo/SP, Brasil
carvalho@ipen.br

Roberto Navarro de Mesquita
Centro de Engenharia Nuclear (CEN)
Instituto de Pesquisas Energéticas e Nucleares (IPEN)
São Paulo/SP, Brasil
rnavarro@ipen.br

2025 16th IEEE International Conference on Industry Applications (INDUSCON) | 979-8-3315-5837-6/25/$31.00 ©2025 IEEE | DOI: 10.1109/INDUSCON66435.2025.11241493

***Abstract*— Predictive maintenance, through regular monitoring of the actual electromechanical condition, efficiency, and other operational indicators of machines and process systems, ensures maximum intervals between repairs and reduces the frequency and cost of unplanned shutdowns caused by failures. Therefore, it is essential to develop efficient methodologies that are feasible for implementation in industrial plants, enabling control and predictability of maintenance downtime. In this context, the Envelope Technique—a reference method for fault analysis, diagnosis, and monitoring in bearings—is applied through frequency-domain spectral analysis of vibration signals, based on the propagation of amplitude near the natural frequency of the component under analysis. This work presents a simple, efficient, and innovative methodology for experimental simulations, monitoring, diagnosis, fault prediction, and estimation of the Remaining Useful Life (RUL) of bearings in rotating machines using vibration signals acquired by a sensor installed on a test bench specifically designed and built to replicate the dynamics of real-world rotating machinery. The implemented experimental simulations generated the progressive increase of vibration peaks—characteristic of fault evolution—through a novel method involving the controlled application of dynamic radial loads. Vibration spectral datasets were collected from an MPU6050 sensor via an Arduino Mega 2560 board, integrated with a model developed in Simulink, which enabled real-time signal acquisition and data file generation for critical (or admissible) fault prediction through processing in MATLAB. The prediction of the critical fault occurrence and RUL estimation was performed using a simple numerical method based on successive function approximation, which allowed the derivation of a characteristic degradation function for the system. Measurements were conducted on both healthy and defect-induced ball bearings under different applied radial loads. The methodology proved efficient and easy to implement in real-world industrial applications, yielding RUL estimates with errors below 25%, and in some cases, as low as 5%. The most accurate RUL predictions were obtained when the signal acquisition rate exceeded 15 times the natural frequency (fn) of the component under study. The procedures developed in this work can be effectively applied in industrial environments to predict the occurrence of critical bearing failures in advance and may be adapted for monitoring other components and systems, including nuclear facilities, enabling accurate and reliable RUL estimation.**

Keywords— Predictive Maintenance, Bearing Fault Diagnosis, Remaining Useful Life (RUL), Vibration Analysis, Envelope Technique.

I. INTRODUCTION

Currently, with advances in electronics, the widespread availability of sensors, and increased computing power—including the application of artificial intelligence techniques such as neural networks—research on failure prediction in rotating machines and their components has significantly expanded. These efforts are primarily based on the monitoring of actual electromechanical operating conditions.

Accurately predicting the moment when a critical failure will occur—necessitating the shutdown of equipment for component replacement or repair—enables maintenance activities to be scheduled at times that minimize disruption to operations or production. The data collected through real-time electromechanical monitoring supports the use of techniques to estimate the Remaining Useful Life (RUL) of systems and/or their components.

In the case of ball bearings, which are the focus of this study, vibration is the most critical parameter. According to [1], the most effective method for condition monitoring is the envelope technique, which relies on spectral analysis to assess the propagation of vibration signal amplitude within a specific frequency range (the "envelope"), typically near the component's natural frequency. This amplitude tends to increase as the fault severity progresses over the course of operation, as illustrated in Figure 1.

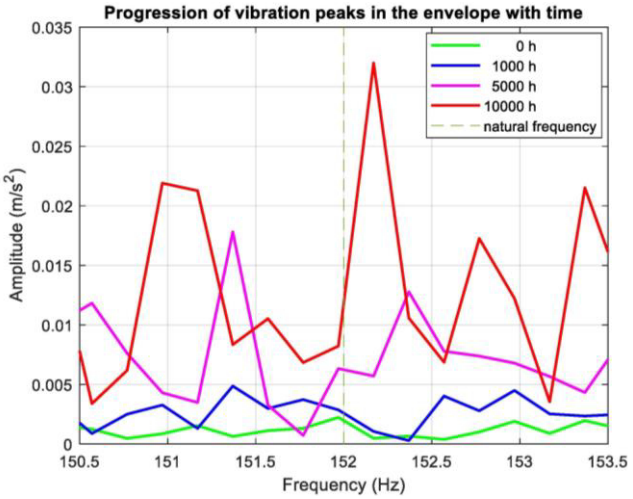

Fig. 1. Growth of vibration peak amplitudes in the envelope frequency band as a function of time, illustrating fault progression in the monitored component

According to Shannon's Sampling Theorem and applying the Nyquist criterion as a practical minimum sampling

condition, the number of signal samples per unit time must be greater than twice the highest frequency component of the signal to allow accurate and error-free reconstruction. In this context, the sampled signal corresponds to the natural frequency of the machine element under analysis [1]. Although the Nyquist criterion defines twice the natural frequency as the minimum sampling rate, it is advisable to use acquisition systems that allow much higher sampling rates—typically ten times the natural frequency—to ensure greater resolution in the frequency spectrum and facilitate the identification and tracking of fault propagation.

II. Literature Review

To develop systems for the analysis, identification, prediction, and monitoring of failures in rotating machinery—as well as for estimating the Remaining Useful Life (RUL) of their components—appropriate data are essential. In the context of this work, vibration signals are used as the primary data source. These signals can be obtained through computational simulations, controlled experiments, or direct acquisition from the equipment or components during operation.

A. Model-based approaches relying on mathematical computational models that simulate real-world electromechanical behavior

First, confirm that you have the correct template for your paper size. This template has been tailored for output on the A4 paper size. If you are using US letter-sized paper, please close this file and download the Microsoft Word, Letter file.

According [3], data-driven prognostics face the persistent challenge of a lack of run-to-failure datasets. In most real-world cases, the available data include failure signatures but little or no information on the progression from the fault's onset to its terminal stage. Acquiring real degradation progression data from electromechanical systems is typically time-consuming and costly. As a result, such systems are rarely instrumented adequately for the collection of relevant data. Furthermore, organizations with access to long-term operational data often restrict public disclosure due to proprietary rights or competitive concerns. Only a few public repositories offer run-to-failure datasets that researchers can use to validate and compare their approaches, limiting progress in the field of fault prognostics.

Mathematical models incorporating functions that describe system degradation dynamics—such as the Weibull model, which is used and detailed in this work—are discussed extensively by Poveda, de Carvalho, and de Mesquita (2025). These models, based on engineered or historically observed features, are applied in simulations of the respective systems they represent, and are also used to predict critical failure or estimate the Remaining Useful Life (RUL). However, such models are limited in their ability to capture anomalous or previously unobserved events. For example, in the referenced work concerning RUL estimation of aircraft engine turbines, simulations are conducted under various operational flight conditions by adjusting parameters such as airspeed and altitude, which affect monitored signals (e.g., temperature, fuel flow, turbine rotational speed). Nevertheless, in a real operational context, if the aircraft encounters unforeseen extreme weather or abrasive volcanic ash—events that are increasingly common—the performance and accuracy of the RUL estimation model may be significantly compromised, impacting maintenance scheduling and system reliability.

B. Condition-Based Monitoring Methods

Although widely studied and well-defined in the literature, current systems and methodologies based on real-time monitoring of electromechanical conditions often fail to provide sufficiently early and accurate predictions of critical failures. These systems typically do not allow for precise temporal forecasting that would enable proactive planning of maintenance shutdowns at ideal times—preferably aligned with the maintenance needs of other components—thus minimizing disruption to the operation of the overall system.

According to [1], one of the most effective approaches for diagnosing and monitoring faults in rotating machinery is vibration analysis in the frequency domain. While time-domain analysis usually does not allow for the early detection of operational anomalies, frequency-domain analysis enables the identification of even minor incipient faults that may indicate the need for future maintenance. This capability arises from the fact that each rotating component subjected to cyclic motion exhibits a characteristic frequency, determined by its design and the frequency of operation.

[1] further emphasizes that condition monitoring relies on the ability to assess the current condition and predict the future state of machines during operation. Every component in standard working condition presents a specific vibration "signature." Over time, as the machine operates, this signature evolves in ways that can be correlated with emerging faults. This concept underpins what is known as mechanical signature analysis.

C. Fault Prediction in Ball Bearings

[4] argue against the validity and effectiveness of broadband time-domain vibration signals for monitoring, diagnosing, predicting, and/or classifying faults in rolling element bearings—particularly when using neural networks—due to the diverse origins of vibration sources. They identify the classical envelope analysis method as the most efficient approach for detecting bearing fault levels. This conclusion can be extended to other rotating components with well-defined characteristic frequencies, such as gear transmissions, pulleys, oscillating elements, unbalanced masses, and similar mechanisms.

Nevertheless, many authors employ broadband spectral data with multiple input variables—either in the time or frequency domain—combined with artificial intelligence techniques (such as simple or convolutional neural networks, fuzzy logic, machine learning, etc.) to detect and classify bearing faults [4].

High-quality bearings typically have long service lives, often spanning thousands of operational hours, even in severe applications. However, this lifespan may vary significantly even for identical components operating under the same machine and system, due to differing severity levels across operational cycles imposed by real-world applications. Therefore, effective fault prediction methodologies for these machine elements must be adaptive to past, present, and future operating conditions. This adaptability is one of the key goals of the present study.

According to [5], localized faults in a ball bearing may occur on the outer race, inner race, cage, or one or more rolling elements. These components, each with distinct natural frequencies, are illustrated in Fig. 2. An increase in vibration amplitude is observed when the rolling elements strike a

localized fault on the outer or inner race, or when a defect on a rolling element comes into contact with the inner or outer race of the bearing.

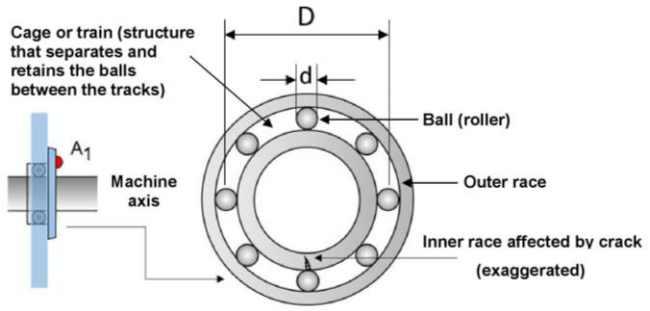

Fig. 2. Bearing and its parts (adapted from [5])

The expressions used to calculate the characteristic fault frequencies of the different components of a ball bearing are given in Equations (1) to (4). As illustrated in Fig. 2, ***d*** is the diameter of the rolling element, and ***D*** is the pitch diameter (mean diameter) of the bearing. The variable f_r represents the shaft rotational speed (in cycles per second or Hz), ***n*** is the number of balls, and φ is the contact angle (equal to 0 for radial bearings) [5].

- Ball Pass Frequency Outer race (BPFO): the natural frequency for fault analysis on the outer race:

$$BPFO = \frac{nf_r}{2}\left(1 - \frac{d}{D}cos\varphi\right) \quad (1)$$

- Ball Pass Frequency Inner race (BPFI): the natural frequency for fault analysis on the inner race:

$$BPFI = \frac{nf_r}{2}\left(1 + \frac{d}{D}cos\varphi\right) \quad (2)$$

- Fundamental Train Frequency (FTF): the natural frequency for fault analysis of the cage:

$$FTF = \frac{f_r}{2}\left(1 - \frac{d}{D}cos\varphi\right) \quad (3)$$

- Ball Spin Frequency (BSF): the natural frequency for fault analysis of the ball.

$$BSF = \frac{Df_r}{2d}\left[1 - \left(\frac{d}{D}cos\varphi\right)^2\right] \quad (4)$$

According to [5], when rolling elements strike localized defects on the outer or inner races, or when defects on the rolling elements come into contact with these races, the resulting impacts produce increases in vibration amplitude at the corresponding characteristic frequencies—BPFO, BPFI, FTF, or BSF—depending on the location of the fault. Therefore, the envelope signal, produced through amplitude demodulation, conveys diagnostic information that is not readily detectable in the raw signal's frequency spectrum analysis.

III. Materials and Methods

A. Fault Simulation Device (FSD) and Its Components

The Fault Simulation Device (FSD) is a test rig designed and built to perform experimental simulations and to support the development of fault prediction techniques. Compared to similar commercial fault simulators, the FSD is more robust and less susceptible to unknown spurious vibrations, which could compromise the methodology for estimating the Remaining Useful Life (RUL). Additionally, it allows for controlled signal superposition, enabling accurate evaluation of performance and reliability in fault detection and prediction.

An overview of the FSD is shown in Fig. 3. Although this study focuses on bearing fault monitoring and prediction, the system was designed to simulate faults in various components and parameters of rotating machinery, including: electric motors, bearings, shaft misalignment, gears, unbalanced mass, pulleys and belts, and energy efficiency.

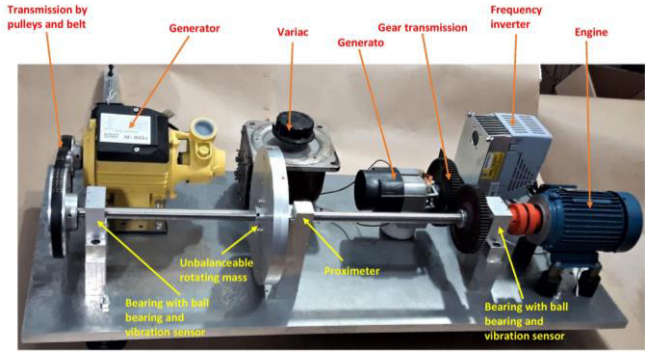

Fig. 3. Fault Simulation Device (FSD)

The different electromechanical components were mounted on a rigid aluminum base with a thickness of 5/8" (~15.9 mm), ensuring a stable system with low susceptibility to external disturbances (spurious vibrations).

The main shaft of the setup, directly driven by a three-phase motor controlled by a frequency inverter, was supported by two bearings mounted at each end of the shaft. The bearings used were SKF 6202-2Z deep groove ball bearings, which are the subject of this study for monitoring, analysis, and fault prediction. The main parameters of these bearings are [6]:

- Ball diameter: d = 6 mm;
- Pitch diameter: D = 25 mm;
- Number of rolling elements: n = 8;
- Contact angle: $\phi = 0$.

For comparative analysis (bearings with and without faults), vibration signals must be collected from both healthy bearings (in perfect working condition) and one or more faulty bearings. To induce a detectable fault in a new bearing, a 4 mm hole was drilled into the outer race, as shown in Fig. 4.

Fig. 4. Bearing with induced fault (hole) in the outer race

Accordingly, the relevant equation for this study is Equation (1), which calculates the Ball Pass Frequency of the Outer Race (BPFO). The shaft rotational frequency f_r, in Hz, was obtained by converting the shaft speed from revolutions per minute (rpm) using Equation (5). The shaft frequency and corresponding BPFO were calculated for each rotational speed used during the experimental simulations.

To measure the vibration signals, an MPU-6050 accelerometer by InvenSense/TDK [7] was selected. This sensor communicates via the I²C protocol and features programmable measurement ranges from ±2g to ±16g. The specified output sampling rate ranges from 4 Hz to 1000 Hz. Its selection was based on availability and a broad body of literature supporting its application in condition monitoring.

The shaft was driven by a three-phase Eberle electric motor [8], rated at 1/4 HP (180 W), 2 poles, with a nominal speed of 3345 rpm. For speed control, a WEG CFW10 frequency inverter [9] was installed, powered by 220 V input and providing a three-phase output to the motor. The inverter allows for speed adjustment in 10 rpm increments and frequency control with a resolution of 0.1 Hz, enabling precise tuning.

B. *Signal Acquisition and Data File Generation*

To acquire the signals from the vibration sensor (accelerometer) installed on the test rig, an Arduino Mega 2560 board (with ATMega328P processor) was used due to its availability and compatibility with Simulink models, which were employed to receive the signals and save the data files. For signal processing, MATLAB/Simulink software (version R2024b) was used because of its relevance and widespread use in research applications, in addition to its advanced capabilities for signal processing and analysis. The sensor was connected to the Arduino Mega 2560 via the I2C bus, as shown in the wiring diagram in Fig. 5.

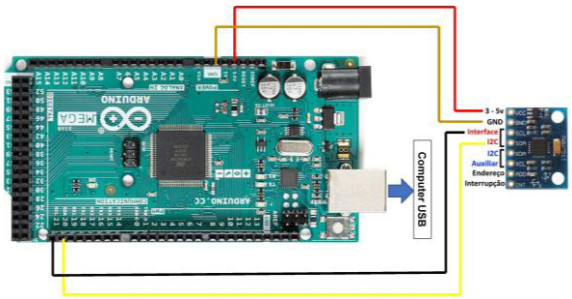

Fig. 5. Arduino connection - MPU6050 accelerometer

Using the MPU6050 Block in the Simulink model developed for signal acquisition and data logging from the vibration sensor connected to the Arduino Mega 2560 board, as shown in Fig. 6, the vibration data can be automatically saved into three separate data files: Acel_x, Acel_y, and Acel_z (corresponding to each of the x, y, and z axes, respectively).

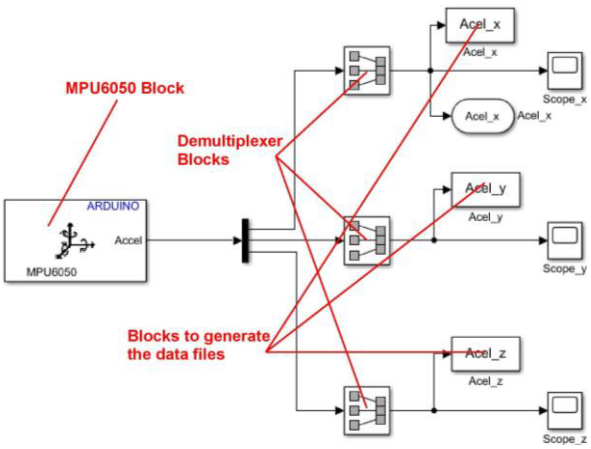

Fig. 6. Simulink model

C. *Experimental Simulation of Fault Progression/Intensification Through the Application of Radial Loads*

The simulation of fault propagation throughout the operation time serves as the foundation for developing a methodology to predict the optimal maintenance stop—intended for replacing the defective component as close as possible to the end of its useful life. This approach aims to maximize component utilization while avoiding unplanned downtime and losses in the production process or equipment operation.

Based on the well-established knowledge that fault propagation in a bearing during the operation of a rotating machine generates progressively higher vibration amplitudes within the envelope frequency band [1], this work proposes a novel methodology to simulate bearing fault progression by applying progressively increasing radial loads.

The application of progressively increasing radial loads generates correspondingly higher vibration amplitudes within the envelope frequency band, closely simulating the behavior observed during real fault propagation in rolling-element bearings of rotating machinery. This innovative methodology, developed and implemented in the present study, enables fault progression to be simulated in a simple and time-efficient manner, eliminating the need for long-term monitoring over thousands of operational hours, as typically required in real-world scenarios.

The direct relationship between the magnitude of the applied radial load and the vibration acceleration measured (in m/s²) can be explained by Newton's Second Law, expressed in Equation (5), and the system dynamics illustrated in Figure 7.

$$F = m \, . \, a \tag{5}$$

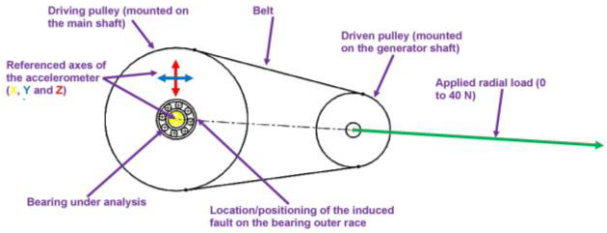

Fig. 7. Pulleys, belt, and applied load

In the system under study, the force ***F*** is the controlled, variable radial load (depicted as the green arrow in Figure 7), and the mass ***m*** is the constant sum of the masses of the assemblies subjected to this force (shaft, bearing elements, pulleys, belt, etc.). Therefore, the greater the applied radial load ***F***, the greater the acceleration ***a*** measured by the accelerometer mounted on the bearing housing, with vibration peaks occurring as the rolling elements pass over the induced fault on the outer race.

To simplify the process and obtain reliable "signatures" of the vibration spectra from both intact (new) and faulty bearings, minimizing spurious vibrations from other components, measurements were taken in two different configurations:

- With the simplified plant configured with only the frequency inverter, motor, main shaft, and associated components (coupling, bearings, pulleys, supports,

etc.), without the rotating mass and other transmission elements such as belts and gears, as shown in Figure 8. This figure also shows the signal acquisition device (Arduino Mega board) that receives signals and sends them to the computer for MATLAB/Simulink processing. In this configuration, the radial (or transverse) load on the bearing can be considered practically zero.

- With the belt and pulley transmission coupled to the generator and radial load applied to the bearing, precisely controlled via a belt tensioner and digital dynamometer, as shown in Figure 9.

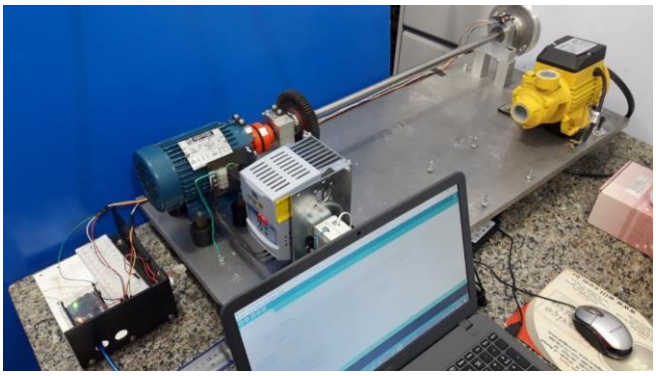

Fig. 8. FSD (with the simplified plant configured), data acquisition system, and computer

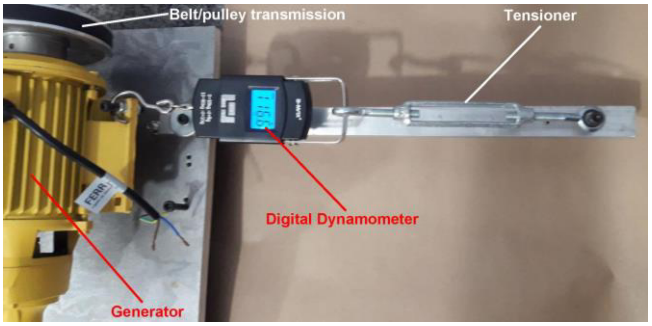

Fig. 9. Belt tensioning system

Progressively increasing radial loads ranging from 0 to 40 N were applied to the bearing with the induced fault in discrete steps of 10 N, resulting in successive increases of vibration peaks within the envelope frequency band around the natural frequency. This phenomenon reflects the typical vibration growth seen in rotating machines as their components degrade due to operational wear.

To make the parameters used more representative of real-world conditions, where system degradation evolves over operating time, the applied loads simulating component degradation were related to time intervals. This allows associating increasing vibration peaks with the component's useful life until reaching a threshold corresponding to catastrophic failure, compromising normal functionality. The Weibull model [10], recognized as a statistical distribution capable of describing different degradation behaviors [2], was employed for this purpose.

The Weibull model is defined by the cumulative distribution function (CDF), expressed as Equation (7) [2]:

$$F(t) = 1 - e^{-\left(\frac{t-t_0}{\eta}\right)^{\beta}} \quad (7)$$

where t is the current time, t_0 is the start time of system operation or the analysis starting point, η is the characteristic life parameter, and β is the shape parameter.

A simpler approach uses the survival function $S(t)$, complementary to the CDF and also known as the Probability Density Function (PDF), expressed as Equation (8) [2].

$$S(t) = 1 - F(t) = e^{-\left(\frac{t-t_0}{\eta}\right)^{\beta}} \quad (8)$$

Estimating the parameters η and β can be done via statistical methods such as maximum likelihood or graphical methods (Weibull plot). MATLAB's "wblfit" function facilitates parameter estimation from failure time data [10]. Using an assigned time vector in hours [500,1000,1500,2000,2500] correlated with the applied load vector in Newtons [0,10,20,30,40], the estimated parameters were η=1414.3478 and β=2.4532.

With these parameters, the survival function curve was plotted using MATLAB's "wblpdf" function, as shown in Figure 10. The figure highlights survival factor indices for each operating time, decreasing from 100% (index 1) at t=0 hours to 1.6% (index 0.016) at t=2500 hours of elapsed operation.

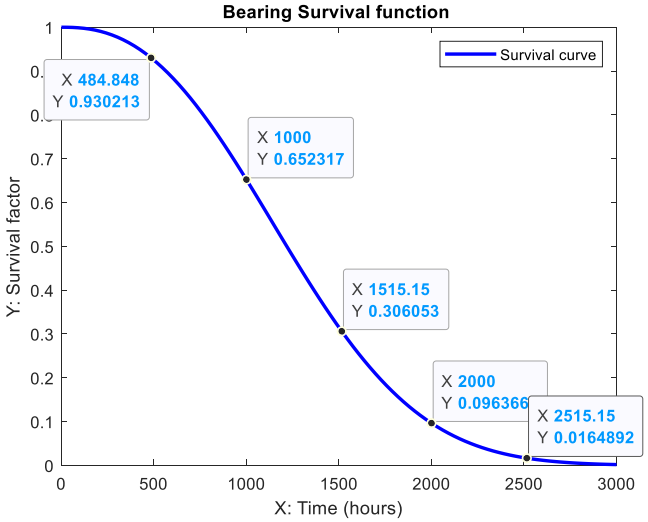

Fig. 10. Survival function obtained from the Weibull degradation model

This methodology proposes establishing a relative load (Cr) from the maximum applied load simulating the failure limit. By assuming a proportional relation between minimum and maximum load intervals per the degradation model, intermediate (relative) loads can be linked to time periods in hours.

The product of the inverse survival factor indices ($1-fs$) and the maximum load of 40 N applied experimentally yields relative loads proportional to this maximum load, as given in Equation (9).

$$Cr = 40(1 - fs) \quad (9)$$

Using this methodology, equivalent times (Te) for each applied load can be calculated by polynomial convergence from relative load times, per Equation (10). The data used for polynomial fitting and the resulting equivalent times are shown in Table I.

$$Te = -0{,}21.C^2 + 60{,}52.C + 179{,}56 \quad (10)$$

TABLE I. RELATIONSHIP BETWEEN APPLIED LOAD AND EQUIVALENT OPERATING TIME BASED ON THE WEIBULL MODEL

Time [hours]	Survivor factor (*fs*)	Relative load (Cr) [N]	Applied load (C) [N]	Equivalent time (*Te*) [hours]
0	1.00	0	0	0
500	0.90	4	0	180
1000	0.65	10	10	760
1500	0.30	28	20	1300
2000	0.05	38	30	1800
2500	0.01	40	40	2260

Figure 11 presents an example result graph relating applied loads and respective vibration peaks within the envelope spectrum to elapsed operating time (in hours) proportional to applied radial loads.

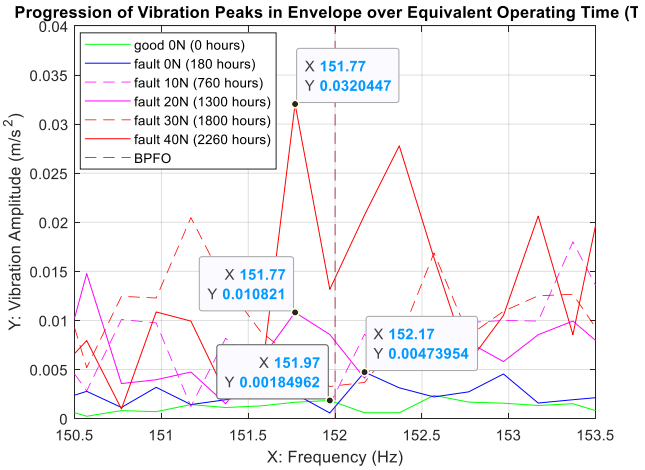

Fig. 11. Example of a result obtained in one of the measurement sequences showing the progression of vibration peaks within the envelope for different applied loads and the corresponding operating periods assigned to simulate the degradation of an outer race bearing fault

The Weibull model used here to determine a time-based pattern (in hours) linked to applied loads (in Newtons) can be replaced by any other suitable degradation progression model based on load application. The key point is that loads are applied progressively over time intervals consistent with real-world degradation processes, thus approximating failure prediction via condition monitoring (measured vibration peaks) to dynamic situations in rotating machinery.

D. Prediction of critical failure occurrence and estimation of remaining useful life (RUL)

To achieve convergence of the characteristic function representing the degradation of the monitored element—in this study, the outer race fault of a bearing—it is necessary to define a fault progression indicator. In this case, the chosen indicator is the amplitude of the maximum vibration peak within the envelope spectrum band. Two different envelope bands were used for condition monitoring in this work: ±1.5% and ±5% around the natural frequency of the analyzed component.

An alternative indicator is the integral of the vibration signal within the envelope band, or in other words, the area under the curve in that spectral region. This integral corresponds to the product of the vibration amplitude measured by the sensor and the frequency. It is also possible to calculate an arithmetic or weighted average of the Remaining Useful Life (RUL) estimates obtained through the convergence of functions based on two or more indicators. The optimal choice depends on the monitored element and the measurement conditions in each case. Both indicators can be used jointly, and the average of their results can be adopted.

In this study, both indicators were employed and evaluated for determining the degradation function of the system using polynomial approximation for convergence.

Finally, an appropriate admissible threshold value must be defined for the chosen indicator. This threshold corresponds to the moment of critical failure occurrence and serves as the reference point for estimating RUL. Depending on the component and the selected indicator, this value may be obtained from the manufacturer's specifications or, more commonly, determined experimentally. In this work, the vibration peak values recorded under an applied radial load of 40 N were used for this purpose.

Three indicators were tested for convergence of the degradation function and RUL estimation at different time intervals (elapsed time): maximum peak within the envelope; integral of the vibration amplitude curve within the envelope; and the arithmetic mean of the RULs estimated from both indicators.

The functions of time as a function of the indicators, obtained through polynomial convergence, are presented in Equations (11) (converged using the maximum peaks within the envelope band) and (12) (converged using the integrals at different time intervals within the envelope band). Throughout the development of this work, it was observed that third-degree polynomials are suitable for representing the system's degradation.

$$t(p) = 354950.p^3 - 20614.p^2 + 539.p \quad (11)$$

$$t(i) = 173350.i^3 - 10769.i^2 + 351.i \quad (12)$$

where ***t*** is the elapsed time, ***p*** is the vibration peak within the envelope spectrum band, and ***i*** is the integral of the vibration amplitude curve within the envelope spectrum band.

The RUL estimates corresponding to each of the system degradation indicator variables are obtained using the expressions shown in Equations (13) and (14).

$$RUL_p = t(max\_p) - t(p) \quad (13)$$

$$RUL_i = t(max\_i) - t(i) \quad (14)$$

where $\boldsymbol{RUL_p}$ is the estimated remaining useful life based on the vibration peaks within the envelope frequency band; $\boldsymbol{t(max_p)}$ is the total predicted time until the occurrence of the maximum admissible peak; $\boldsymbol{t(p)}$ is the elapsed time at the moment of prediction (RUL estimate) based on vibration peaks; $\boldsymbol{RUL_i}$ is the estimated remaining useful life based on the integral of the vibration peaks within the envelope frequency band; $\boldsymbol{t(max_i)}$ is the total predicted time until the occurrence of the maximum admissible value for the integral of the vibration peaks; and $\boldsymbol{t(i)}$ is the elapsed time at the moment of prediction (RUL estimate) based on the integral of vibration peaks.

The graph in Figure 12 illustrates an example of results obtained for the RUL estimates in one of the measurements performed.

The diagram shown in Figure 13 presents the algorithm developed and employed for automated prediction of critical failure occurrence and RUL estimation, without the need for analyst intervention. The process begins with the input of

vibration signals, followed by the application of the envelope technique, which serves as the basis for extracting degradation indicators of the component under analysis. These indicators are used for the convergence of the function representing the fault evolution process, resulting in the estimation of the remaining useful life, which is the output parameter of the implemented program.

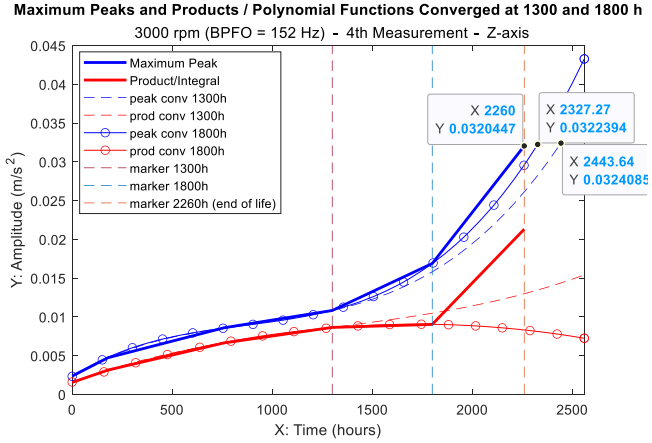

Fig. 12. Graph showing maximum peaks and products within the envelope frequency band and RUL estimates through polynomial convergence

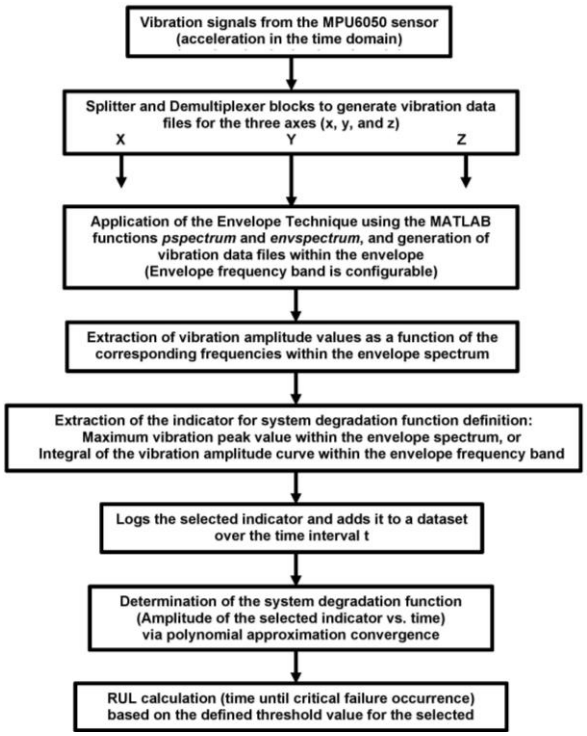

Fig. 13. The algorithm to RUL estimation

IV. Results

Spectral signal acquisitions were carried out using the vibration sensor positioned at one of the bearings on the main shaft of the plant, both under healthy (fault-free) and induced fault conditions. Data were collected along the three axes (x, y, and z), in 5-second cycles, under varying conditions—shaft rotational speeds, radial loads, and signal acquisition rates.

Five measurements were performed for each operating condition, resulting in five datasets per condition. The developed Simulink model allowed vibration data files for each axis to be saved in ".mat" format, simplifying signal processing through MATLAB programs using the envelope analysis technique.

Envelope signals were extracted under the various test conditions, and the corresponding spectral signatures were obtained from experimental simulations of the plant under both healthy and faulty bearing conditions. Radial loads applied were 0 N (no load), 10 N, 20 N, 30 N, and 40 N, and shaft rotational speeds were set at 302, 599, 901, 1200, 1800, and 3000 rpm, controlled via the frequency inverter installed in the system. Vibration signals were also acquired at different sampling rates: 100 Hz, 200 Hz, 500 Hz, and 1000 Hz.

In total, 1,500 vibration data files were generated and analyzed.

For a total simulated/expected useful life of 2260 hours, RUL estimations were performed at 1300 hours (~58% of the total life), corresponding to an expected remaining life of 960 hours, and at 1800 hours (~80% of the total life), corresponding to an expected remaining life of 460 hours. To classify the accuracy of the predictions, an error margin of up to 25% between the estimated and expected RUL values was adopted. Estimations falling within this margin—highlighted in yellow in the tables—were considered satisfactory and indicative of predictive effectiveness.

Table II presents the RUL estimation results obtained through polynomial convergence based on vibration peak amplitudes within the envelope frequency range. For rotational speeds above 1200 rpm, due to the signal acquisition rate limitation of 1000 Hz imposed by the hardware, it was not possible to capture the relevant vibration features (i.e., peaks within the envelope spectrum) with sufficient resolution and precision to characterize the degradation processes and produce reliable polynomial convergence for accurate RUL estimations.

TABLE II. Predictions of RULs Based on the Progression of Vibration Peaks

Rotational Speed (rpm)	Ref. Axis	Measurement	Estimated RULs Based on Peak Vibration Limits Within the Envelope Spectrum (fn ± 5%), Using 1000 Hz Acquisition Rate					
			RUL Estimates at 1300 h (Actual RUL: 960 h)			RUL Estimates at 1800 h (Actual RUL: 460 h)		
			RUL (hours)	Abs. error (hours)	Relative error (%)	RUL (hours)	Abs. error (hours)	Relative error (%)
901	y	1st	993	53	5.6	493	33	7.2
		2st	776	-164	-17.4	356	-104	-22.6
		3st	990	50	5.3	566	106	23.0
		4st	1011	71	7.6	511	51	11.1
		5st	758	-182	-19.4	363	-97	-21.1
		Mean	**906**	**-34**	**-3.7**	**458**	**-2**	**-0.5**
	z	1st	n.a.	n.a.	n.a.	n.a.	n.a.	n.a.
		2st	953	13	1.4	438	-22	-4.8
		3st	908	-32	-3.4	796	336	73.0
		4st	1455	515	54.8	1024	564	122.6
		5st	n.a.	n.a.	n.a.	n.a.	n.a.	n.a.
		Mean	**1105**	**165**	**17.6**	**753**	**293**	**63.6**
1200	y	1st	1342	402	42.8	813	353	76.7
		2st	1269	329	35.0	823	363	78.9
		3st	1250	310	33.0	751	291	63.3
		4st	1149	209	22.2	649	189	41.1
		5ª	1926	986	104.9	793	333	72.4
		Mean	**1387**	**447**	**47.6**	**766**	**306**	**66.5**
	z	1st	1223	283	30.1	711	251	54.6
		2st	1127	187	19.9	648	188	40.9
		3st	1141	201	21.4	641	181	39.3
		4st	978	38	4.0	532	72	15.7
		5st	1057	117	12.4	598	138	30.0
		Mean	**1105**	**165**	**17.6**	**626**	**166**	**36.1**

Table II presents the RUL estimation results obtained through polynomial convergence based on the integrals (areas under the curve) of the vibration amplitude within the

envelope frequency range. In these cases, consistent and satisfactory results (highlighted in yellow) were obtained under the same 25% error criterion.

TABLE III. PREDICTIONS BASED ON THE INTEGRALS OF VIBRATION CURVES WITHIN THE ENVELOPE SPECTRUM

Rotational Speed (rpm)	Ref. Axis	Measurement	Estimated RUL Results Based on the Admissible Limit of the Integral Within the Envelope Spectrum (fn ± 5%), Using 1000 Hz Acquisition Rate					
			RUL Estimates at 1300 h (Actual RUL: 960 h)			RUL Estimates at 1800 h (Actual RUL: 460 h)		
			RUL (hours)	Abs. error (hours)	Relative error (%)	RUL (hours)	Abs. error (hours)	Relative error (%)
901	y	1st	3992	3052	324.7	994	534	116.1
		2st	2770	1830	194.7	766	306	66.5
		3st	990	50	5.3	490	30	6.5
		4st	1002	62	6.6	511	51	11.1
		5st	1053	113	12.0	736	276	60.0
		Mean	**1961**	**1021**	**108.7**	**699**	**239**	**52.0**
	z	1st	751	-189	-20.1	703	243	52.8
		2st	1016	76	8.1	619	159	34.6
		3st	1267	327	34.8	1598	1138	247.4
		4st	1444	504	53.6	3968	3508	762.6
		5st	1182	242	25.7	682	222	48.3
		Mean	**1132**	**192**	**20.4**	**1514**	**1054**	**229.1**
1200	y	1st	1232	292	31.1	776	316	68.7
		2st	1303	363	38.6	809	349	75.9
		3st	1214	274	29.1	713	253	55.0
		4st	1297	357	38.0	803	343	74.6
		5st	1734	794	84.5	854	394	85.7
		Mean	**1356**	**416**	**44.3**	**791**	**331**	**72.0**
	z	1st	1106	166	17.7	606	146	31.7
		2st	872	-68	-7.2	410	-50	-10.9
		3st	1040	100	10.6	540	80	17.4
		4st	973	33	3.5	473	13	2.8
		5st	937	-3	-0.3	447	-13	-2.8
		Mean	**986**	**46**	**4.9**	**495**	**35**	**7.7**

In the tables, entries marked with "n.a." (not available) indicate that a coherent degradation trend could not be identified—e.g., resulting in negative RUL estimates, which are physically non-meaningful and thus discarded.

CONCLUSIONS

The methodology proposed and developed in this study has proven effective for the automated estimation of Remaining Useful Life (RUL) of components, without the need for human intervention. The approach relies on the extraction of degradation indicators from the envelope spectrum of vibration signals and the application of polynomial curve fitting to model the degradation evolution.

Despite the limitations imposed by the data acquisition system—particularly the maximum sampling rate of 1000 Hz—it was possible to obtain accurate RUL estimates under operating conditions with shaft rotational speeds up to 1200 rpm. For higher speeds, it became evident that increased sampling frequencies are required to accurately capture vibration peaks within the envelope spectrum.

In the case under analysis, a rotational speed of 1200 rpm corresponds to a natural frequency (fn) of 60.8 Hz for the bearing's outer ring. Based on this, it can be concluded that the sampling frequency should be at least 15 times higher than the natural frequency of the component under monitoring to ensure reliable signal resolution.

The results confirm the feasibility of the proposed approach for application in real-world condition monitoring systems, provided that the minimum requirements for signal quality and resolution are met.

The polynomial convergence methodology developed in this study for Remaining Useful Life (RUL) estimation - based on degradation process indicators such as vibration peaks or the integral of the vibration envelope spectrum - presents two key advantages over widely adopted approaches such as Artificial Neural Networks (ANNs), detailed and compared in [11]:

- Adaptivity: The method is inherently adaptive and sensitive to variations in the severity of operating conditions over time. As such, it can be applied to different components subjected to various operational environments and degradation mechanisms.
- Improved Accuracy Over Time: The accuracy of RUL predictions improves progressively as the component approaches the end of its useful life, asymptotically tending toward 100% accuracy near the failure threshold.

The proposed algorithm operates in a fully automated manner, from vibration signal acquisition to RUL estimation, eliminating the need for manual analysis.

Throughout this study, the proposed methodologies—both for experimental simulations of fault evolution through the application of progressively increasing radial loads, and for fault prediction and Remaining Useful Life (RUL) estimation using successive function convergence—proved to be more efficient and innovative compared to conventional approaches reported in the literature.

REFERENCES

[1] R. B. Randall, Vibration-based Condition Monitoring: Industrial, Aerospace and Automotive Applications. Chichester, U.K.: John Wiley & Sons Ltd, 2011.

[2] NIST/SEMATECH, e-Handbook of Statistical Methods, 2012. [Online]. Available: http://www.itl.nist.gov/div898/handbook/. [Accessed: Nov. 2023]. DOI: https://doi.org/10.18434/M32189

[3] A. Saxena, K. Goebel, D. Simon, and N. Eklund, "Damage propagation modeling for aircraft engine run-to-failure simulation," in 2008 PHM, Denver, CO, USA, 2008. [Online]. Available: https://ieeexplore.ieee.org/document/4711414. [Accessed: Nov. 2023].

[4] R. B. Randall and J. Antoni, "Rolling element bearing diagnostics—A tutorial," Mech. Syst. Signal Process., vol. 25, pp. 485–520, 2011.

[5] MathWorks, "Rolling Element Bearing Fault Diagnosis." [Online]. Available: https://www.mathworks.com/help/predmaint/ug/Rolling-Element-Bearing-Fault-Diagnosis.html. Accessed: Feb. 2022.

[6] SKF, Deep Groove Ball Bearing 6202-2Z. Available: https://www.skf.com/br/products/rolling-bearings/ball-bearings/deep-groove-ball-bearings/productid-6202-2Z. Accessed: Feb. 2022.

[7] InvenSense Inc./TDK, MPU-6000 and MPU-6050 Product Specification, Rev. 3.4. Sunnyvale, CA, USA, 2022. [Online]. Available: https://product.tdk.com/system/files/dam/doc/product/sensor/mortion-inertial/imu/data_sheet/mpu-6000-datasheet1.pdf. Accessed: Aug. 2022.

[8] EBERLE, Three-Phase Electric Motors – Industrial and High Efficiency. Eberle, a Metalcorte Company, Sep. 2005. [Online]. Available: https://www.bernabeig.com.ar/descargas/ALTO-RENDIMIENTO.pdf. Accessed: Feb. 2022.

[9] WEG, CFW-10 Frequency Inverter – User Manual, May 2013. [Online]. Available: https://static.weg.net/medias/downloadcenter/h0d/h99/WEG-cfw10-manual-do-usuario-0899.5860-2.xx-manual-portugues-br.pdf. Accessed: Feb. 2022.

[10] MATHWORKS, "Weibull Distribution." Available: https://www.mathworks.com/help/stats/weibull-distribution.html. Accessed: Nov. 2023.

[11] C. Zhang, P. Lim, A.K. Qin, and K.C. Tan. "Multiobjective deep belief networks ensemble for remaining useful life estimation in prognostics". IEEE Trans Neural Netw Learn Syst 2017; 28(10):2306–18. https://doi.org/10.1109/TNNLS.2016.2582798.